Supplementary Information

High-throughput mechanical nuclear envelope rupture and the intracellular dynamics of massive wound repair

Apresio K. Fajrial,[a,1] Leyla Akh,[b,1] Stephanie E. Schneider,[a] Benjamin Seelbinder,[a] Xin Xu,[a] Wei Tan,[ab] Corey P. Neu,[abc] Xiaoyun Ding.[abc*]

[a] Paul M. Rady Department of Mechanical Engineering, University of Colorado, Boulder, CO 80309, USA.
[b] Biomedical Engineering Program, University of Colorado, Boulder, CO 80309, USA.
[c] BioFrontiers Institute, University of Colorado, Boulder, CO 80309, USA.
[1] Authors contributed equally to this work.
* Corresponding author: Xiaoyun Ding
Email: xiaoyun.ding@colorado.edu

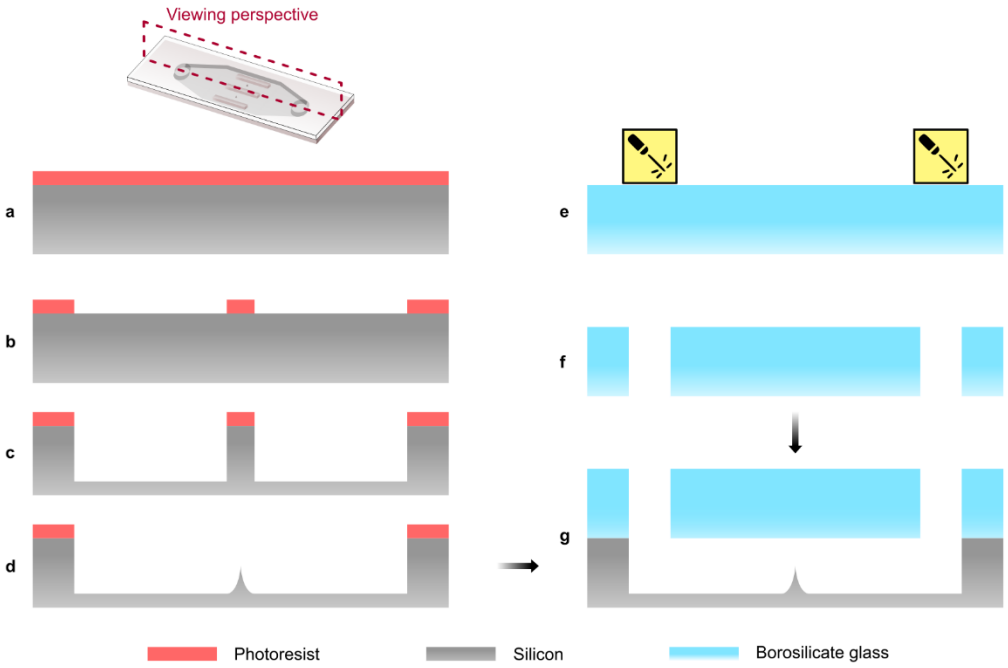

Supplementary Figure 1 | Fabrication process workflow of the NEST device. a-d, Fabrication of sharp tip nanostructure in microchannel on silicon substrate consists of photolithography, deep reactive ion etching, and isotropic etching from a combination of oxide growth and BOE. **e-f**, Inlet and outlet holes fabrication using laser engraver on a borosilicate glass substrate. **g**, Anodic bonding of the silicon and glass substrate with aligned inlet/outlet position.

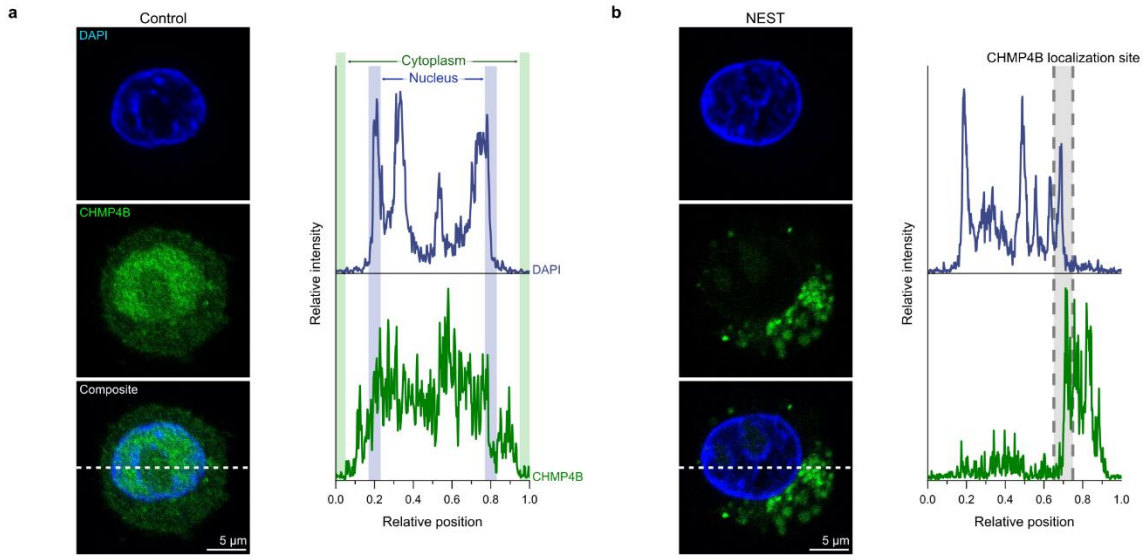

Supplementary Figure 2 | CHMP4B intensity profile from confocal fluorescence images. 3D confocal volume reconstruction of HeLa CHMP4B-GFP cells after NEST treatment. a, Confocal microscopy image of untreated CHMP4B HeLa cells and quantification of the fluorescent intensity profile. Relative positions 0.0 and 1.0 indicate two ends of the cell plasma membrane. **b**, Confocal microscopy image of NEST-treated CHMP4B HeLa cells. CHMP4B proteins aggregate and localize around the boundary between the nuclear envelop and cytoplasmic space (shaded gray region).

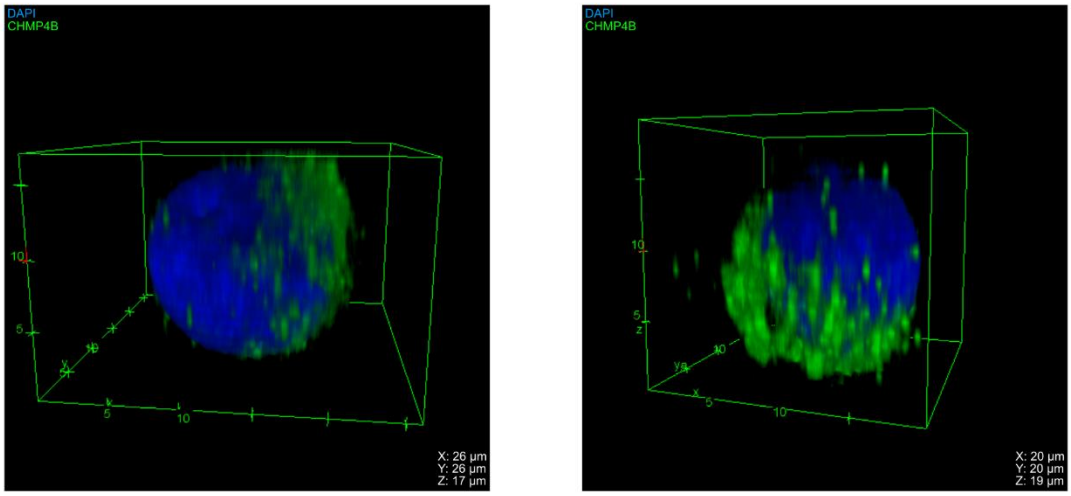

Supplementary Figure 3 | 3D confocal volume reconstruction of HeLa CHMP4B-GFP cells after NEST treatment. The left and right figures are two representative samples showing localized CHMP4B aggregation at a single concentrated area on the nuclear envelope.

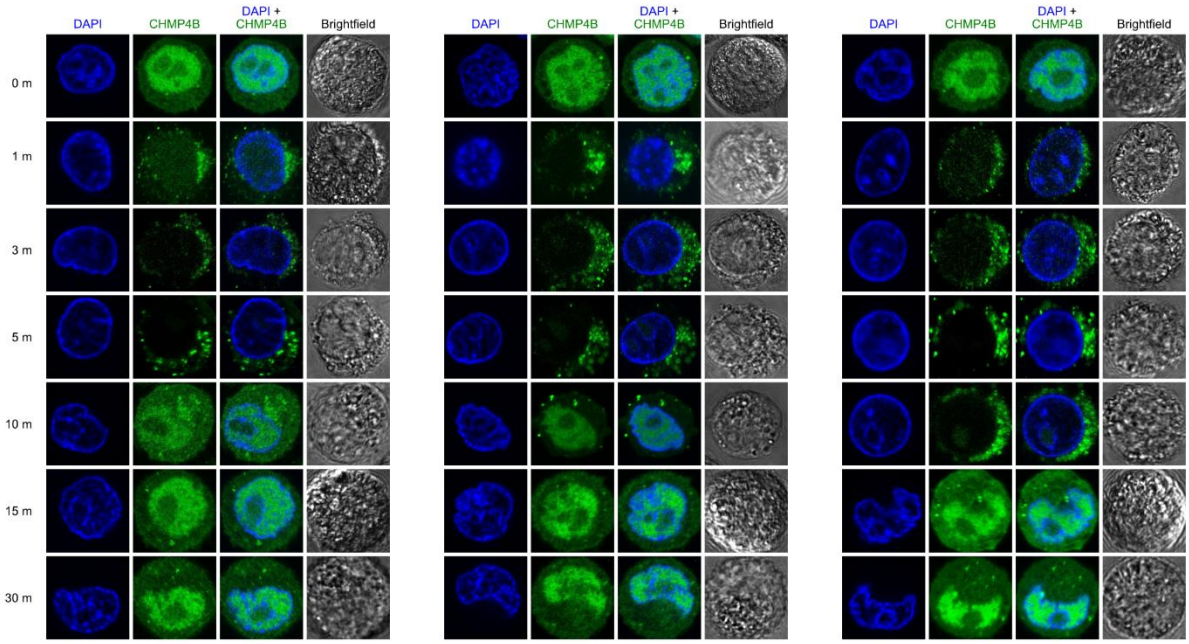

Supplementary Figure 4 | Dynamics of ESCRT-III recruitment on the nuclear envelope after NEST treatment. Representative images of HeLa cells expressing CHMP4B protein, a subunit of ESCRT-III complex, at time points 0, 1, 3, 5, 10, 15, and 30 m after NEST treatment. Large aggregates of CHMP4B proteins were localized at the nuclear surface at time points 1, 3, and 5 m. The CHMP4B protein mainly resided on the cytoplasm side of the puncture, not the nucleoplasm space. CHMP4B protein distribution returns to baseline state at time points 15 m.

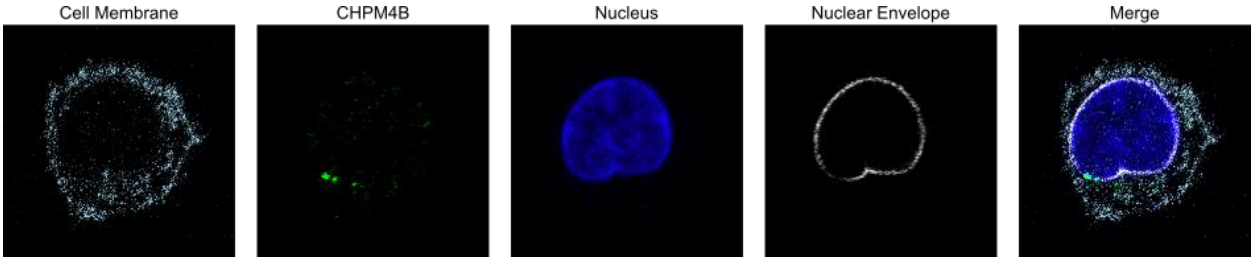

Supplementary Figure 5 | CHMP4B aggregation at the site of nuclear damage. Representative confocal microscopy images of a cell with a ruptured membrane showing CHMP4B aggregation at the site of membrane rupture.

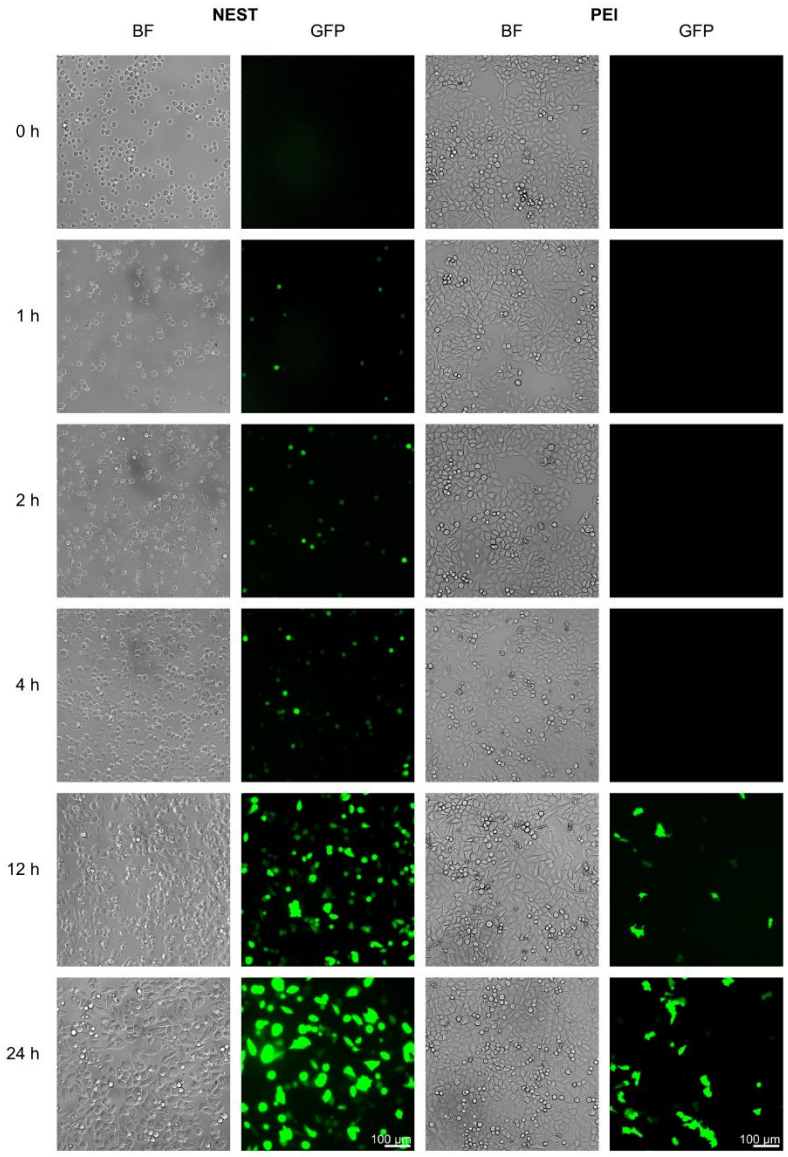

Supplementary Figure 6 | Fluorescence microscopy images of EGFP transfected cells using NEST and PEI methods. The images were recorded at time points 0, 1, 2, 4, 12, and 24 hours as shown in the figure.

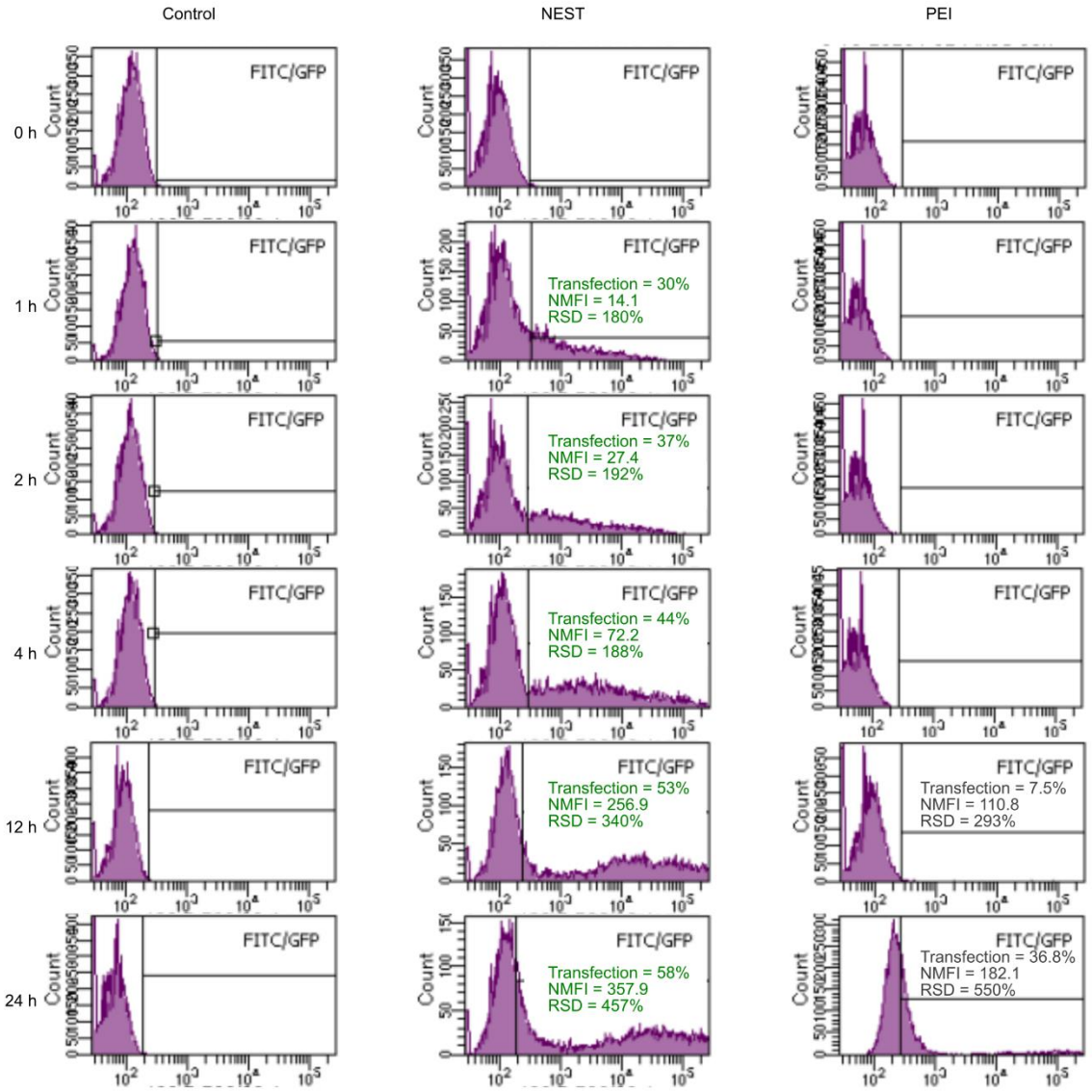

Supplementary Figure 7 | Transfection efficiency assessment of the various intracellular delivery methods using flow cytometry. The expression of plasmid DNA at time points 0, 1, 2, 4, 12, and 24 h is shown in the figure.

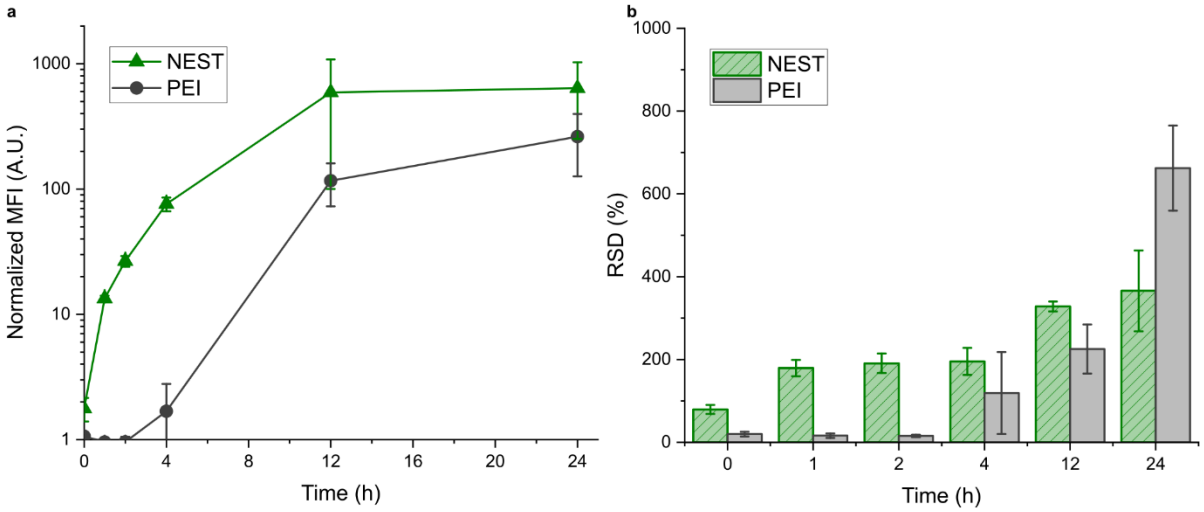

Supplementary Figure 8 | Quantitative assessment of flow cytometry data from EGFP transfected cells using NEST and PEI methods at time points 0, 1, 2, 4, 12, and 24 hours. a, Normalized Mean Fluorescence Intensity (MFI) **b,** Relative Standard Deviation (RSD)**.** Error bars represent s.d. (n = 3)

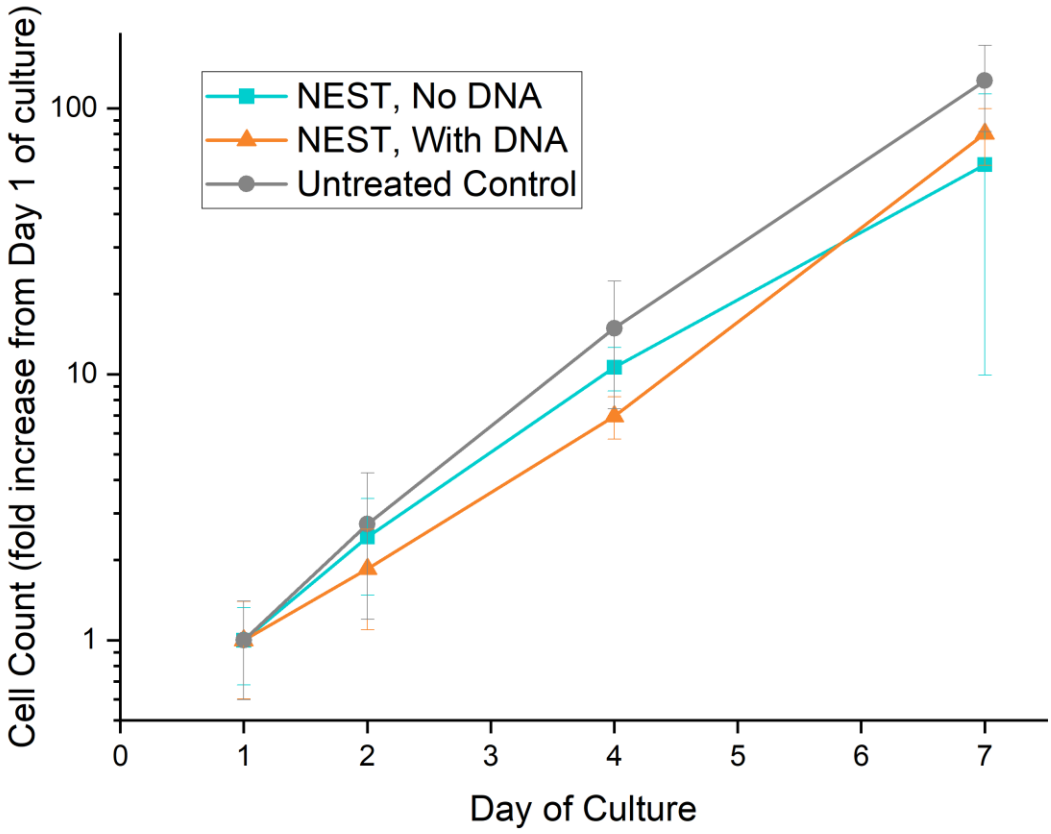

Supplementary Figure 9 | Normalized proliferation of HeLa cells after NEST treatment. Cells were treated with the NEST device, with or without plasmid DNA. At each time point, several representative images were taken of each well of cells. The cells were manually counted in each image using ImageJ. All curves follow an exponential trendline with an R^2 greater than 0.998. Error bars represent s.d. (n=9).